

Thermal wave physics: principles and applications to the characterization of liquids

Ernesto Marín¹

CICATA-IPN, Legaria 694, Col. Irrigación,

México D.F., C.P. 11500, México

(Recebido: 28 de novembro de 2004)

Abstract: This paper describes the concept and principal features of thermal waves using a phenomenological approach. The role played by thermal waves in photothermal techniques is explained using different examples, ranging from the so-called purely thermal wave interferometry to photoacoustic spectroscopy. Some examples concerning the optical and thermal characterization of liquids and their application are presented.

Key words: Thermal waves, photothermal techniques, photoacoustic, thermal properties, thermal effusivity, thermal diffusivity

Resumo: Neste trabalho se descreve o conceito de ondas térmicas e suas principais características por meio de uma aproximação fenomenológica. Explica-se o papel jogado por estas ondas nas técnicas fototérmicas através de vários exemplos, que vão desde a denominada interferometria de ondas térmicas até espectroscopia fotoacústica. Mostram-se também vários exemplos relacionados com a caracterização térmica e óptica de líquidos e suas aplicações.

Palavras-chave: ondas térmicas, técnicas fototérmicas, fotoacústica, propriedades térmicas, efusividade térmica, difusividade térmica

¹Permanent address: Facultad de Física, Universidad de la Habana, san Lázaro y L, Vedado 10400, La Habana, Cuba

E-mail: emarin@fisica.uh.cu, emarin63@yahoo.es

1 Introduction

The conduction of heat is a diffusion-like process, where the thermal energy, in the case of solids, is mainly transported by phonons, the quanta of lattice vibrations, and/or free electrons. In the case of fluids (i.e. liquids and gases) this process occurs through the movement of atoms and molecules in a more complicated form due to the presence of other hydrodynamic effects, such as heat convection.

It has been shown by many authors that the diffusion of thermal energy in a periodically heated material is well described in terms of thermal waves. These waves have become of great interest for the explanation of the photoacoustic (PA) effect and other photothermal (PT) phenomena, on which many non-destructive measurement techniques are based [1]. The PA and PT techniques represent a group of high-sensitivity methods based on a photo-induced change in the thermal state of a sample. The periodic absorption of energy without re-emission losses leads to sample heating, which at the same time induces changes in temperature-dependent parameters of the sample itself and/or of the surrounding medium. The detection of these changes is the basis of the different experimental techniques from which many applications are reported in the last 30 years [1].

Despite the growing interest, the application of PT methods to liquids characterization, which is of considerable interest in several fields, for example in environmental studies, has remained limited, in comparison with studies in the solid and gas phase. This is somewhat contradictory since the modern history of the PT science began with the works of Rosencwaig [2] related, among other applications, to (qualitative) measurement of absorption spectra of some liquid samples, such as blood. Since then, most of the work with liquids involved remote refractive index modulation techniques, such as the PT phase shift technique [3], thermal lens [4] and PT optical beam deflection [5]. More recently, so called open methods have been used successfully in several applications, such as the Piezoelectric Optothermal Window (OW) [6] for spectroscopic measurements and the Photopyroelectric (PPE) method [7-13] for thermal characterization and phase transition detection. In this work we will discuss the use of novel alternative experimental variants for measurement of optical and thermal properties of liquids, namely the Thermal Wave Interferometry (TWI), a technique based so far in PPE detection of thermal waves propagating through the sample, and an open cell PA configuration.

Due to the fact that in the PT methods the heat sources follow the periodic modulation of the excitation light beam, many authors have adopted the principles of wave physics that have been used in the explanation of other periodic phenomena to interpret their experimental results. The wave treatment of heat propagation is also used to demonstrate the occurrence of phenomena that may be regarded as reflection, refraction, interference, and scattering effects in PA and PT experiments [1, 14], as we will see in the next section.

This paper is organized as follows: Firstly the mathematics underlying the thermal wave concept will be described, as well as some historical facts and basic experiments, including the recent proposed technique based in thermal wave interference and its application to thermal characterization of liquids. In section 3 the features of one of the most successful techniques based in thermal waves, namely the photoacoustic method, will be described and the criteria for neglecting convective effects when doing with liquid samples will be derived. Some recent applications concerning the detection of low amounts of contaminants (or dopants) in water, and thermal characterization of liquids will be presented too, with conclusions in section 4.

2 Thermal wave physics

2.1 Historical remarks

In the PT techniques thermal waves are generated in a given sample by means of a periodically varying heat source. Suppose that the time-duration of the light pulses is much larger than the relaxation time of the system (the build-up time necessary for the onset of a heat flux after a temperature gradient is imposed on a sample) so that the parabolic heat diffusion equation can be used successfully [15]. The changes in samples temperature or in temperature depending parameters can be monitored. These changes depend, among others, on the optical and the thermal properties of the samples material. Therefore, among their several applications, one active area of research nowadays is devoted to their use for the optical and thermal characterisation of materials [16]. Although Angstrom in 1861 proposed a temperature-wave method for measuring the thermal diffusivity of a solid in a form of a rod [17], it was not until the 1970s that practical applications of PT techniques have appeared motivated mainly by the works of Alan Rosencwaig [2, 18] in a new emerging field of Photoacoustic Spectroscopy (PAS), a technique based in the Photoacoustic (PA) effect, discovered approximately one century before by Alexander Graham Bell [19], and investigated by relevant scientists of that times such as Röntgen [20], Tyndall [21] and Rayleigh [22] (It is worth to remember the early work of Viengerov in the 1930s [23] dealing with the so-called optoacoustic effect in gases, a field of active current investigation [1]). Consequently with the development of PAS and other PT techniques, the use of a wave treatment of heat dates from the 1980s [24], although the concept of thermal wave was first appeared about hundred years before when Fourier [25] showed that expanding temperature distributions as series of waves could solve heat conduction problems. Fourier, as well as Poisson, have used equations identical to those used today in describing thermal waves in order to estimate the thermal properties at the earth crust, making use of the daily periodical temperature oscillations [25, 26].

In what follows we will briefly present a mathematical appraisal of thermal waves, before describing an experiment based in Fouriers proposals. Although this paper is mainly concerned with applications in the liquid phase, we will initially limit the general analysis to the case of solid materials. Then, in section 3, special features concerning the work with liquids will be discussed.

2.2 The mathematics of thermal waves

In this section we will follow a phenomenological approach to describe the basic features of thermal waves. A more analytical approach, leading to the same results, can be found for example in Mandelis [27]. The starting point will be the heat diffusion equation. Consider an isotropic homogeneous semi-infinite solid, whose surface is heated uniformly (in such a way that the one-dimensional approach used in what follows is valid) by a light source of periodically modulated intensity $I_0(1 + \cos(\omega t))/2$, where I_0 is the intensity of the light source, $\omega = 2\pi f$ is the angular modulation frequency, and t is the time. The temperature distribution $T(x, t)$ within the solid can be obtained by solving the homogeneous heat diffusion equation, which can be written as

$$\frac{\partial^2 T(x, t)}{\partial x^2} - \frac{1}{\alpha} \frac{\partial T(x, t)}{\partial t} = 0, x > 0, t > 0 \quad (1)$$

with the boundary condition

$$-k \frac{\partial T(x, t)}{\partial x} \Big|_{x=0} = \text{Re} \left[\frac{I_0}{2} \exp(i\omega t) \right] \quad (2)$$

which express that the thermal energy generated at the surface of the solid (for example by the absorption of light) is dissipated into its bulk by diffusion.

In the above equations $i = (-1)^{1/2}$ is the imaginary constant and α is the thermal diffusivity and k is the thermal conductivity, related to other important thermal parameters through

$$\varepsilon = \sqrt{k\rho c} = \frac{k}{\sqrt{\alpha}} = \rho c \sqrt{\alpha} \quad (3)$$

where, ε is the thermal effusivity, ρ the density and c the specific heat. The product $C = \rho c$ is referred as the specific Heat Capacity or as Heat capacity per unit volume. An extended explanation of the physical relevance of these parameters, governing the generation and propagation of heat in solids, can be found in many books, monographs, and articles to which the reader can be referred [1, 14, 28-30]. It is worth to remember only that the specific heat, with characterizes the materials ability to store heat, describe static problems, where temperature is independent on time and position, whereas the conductivity is the one required when leading with steady problems, i.e. when the temperature does not vary over time. Thermal conductivity is defined by the Fourier's law [28] of heat conduction, which in one dimension poses

$$q(x, t) = -k \frac{\partial T(x, t)}{\partial x} \quad (4)$$

where $q(x, t)$ is the heat flux and $T(x, t)$ the temperature field, both dependent on time, t , and position, x , coordinates. Thermal conductivity measures, therefore, the heat flowing in unit time through a unit area of a unit thickness material with a temperature difference of one degree between its opposite faces [29].

A time-varying phenomenon, on the other hand, is described by the differential equation of heat diffusion (energy conservation law), as given by Eq. (1), also requiring the knowledge of thermal diffusivity and effusivity. The former is the quantity associated with the speed of propagation of heat in a material during time changes of its temperature, while the thermal effusivity measures the material's ability to exchange heat with the environment and the thermal inertia of a material, as will be seen later.

The solution of physical interest of the problem given by Eqs. (1) and (2) for applications in PT techniques is the one related to the time dependent component. If we separate this component from the spatial distribution, the temperature can be expressed as:

$$T(x, t) = \text{Re} [\Theta(x) \exp(i\omega t)] \quad (5)$$

Substituting in Eq. (1) we obtain

$$\frac{d^2\Theta(x)}{dx^2} - q^2\Theta(x) = 0 \quad (6)$$

where

$$q = \sqrt{\frac{i\omega}{\alpha}} = (1+i)\sqrt{\frac{\omega}{2\alpha}} = \frac{(1+i)}{\mu} \quad (7)$$

and

$$\mu = \sqrt{\frac{2\alpha}{\omega}} \quad (8)$$

The general solution of Eq. (6) using the condition (2) has the form

$$\Theta(x) = \frac{I_0}{2\varepsilon\sqrt{\omega}} \exp\left(-\frac{x}{\mu}\right) \exp\left[-i\left(\frac{x}{\mu} + \frac{\pi}{4}\right)\right] \quad (9)$$

This equation has the meaning of a plane wave. Like other waves it has an oscillatory spatial dependence of the form $\exp(iqx)$, with a wave vector q given by Eq. (7). Because it has several wave-like features, Eq. (9) represents a thermal or temperature wave propagating with phase velocity v_f given by:

$$v_f = \omega\mu = \sqrt{2\alpha\omega} \quad (10)$$

The parameter μ represents the thermal diffusion length of the thermal wave, i.e. the distance at which the propagated wave amplitude decays e times its value at $x = 0$. As can be seen from Eq. (8), it depends on the thermal diffusivity and on the light modulation frequency. Eq. (9) represents, therefore, an attenuated wave. For a given sample the attenuation of a propagating thermal wave varies following the changes in the periodicity of the heat source. The product $2\pi\mu$ is the thermal wavelength. Between the light excitation and the thermal response of the sample there is a phase-lag given by the term $(x/\mu + \pi/4)$ in the complex exponent.

Since Eq. (6) is a linear ordinary differential equation describing the motion of a thermal wave, then the superposition of solutions will be also a solution of it. This superposition represents a group of waves with angular frequencies in the interval $\omega, \omega+d\omega$ travelling in space with a group velocity:

$$v_g = \frac{1}{\frac{dq_R}{d\omega}} = 2\sqrt{2\alpha\omega} = 2v_f \quad (11)$$

where $q_R = \text{Re}(q)$.

2.3 An experiment based in thermal wave propagation in soils

The following is a simple example of a PT experiment. The surface of the earth is exposed to more or less regular daily temperature fluctuations, owing to different causes, that can differ appreciable from day to day, from season to season and from region to region. As a consequence, air and soil temperatures generally exhibit a diurnal cycle with a period $T = 2\pi/\omega$ of near 24 hours. From Eqs. (10) and (6) we can obtain the temperature variations $T(x, t)$ with time, t , and with depth below the surface, x , i.e.,

$$T(x, t) = \frac{I_0}{2\varepsilon\sqrt{\omega}} \exp\left(-\frac{x}{\mu}\right) \text{Re} \left\{ \exp \left[-i \left(\frac{x}{\mu} + \omega t + \frac{\pi}{4} \right) \right] \right\} \quad (12)$$

Measuring $T(x, t)$ as a function of time t at different distances x from the earth surface and fitting the results to Eq. (12), allow ones the determination of parameters like the period of the temperature oscillations, the soils thermal diffusion length and its thermal diffusivity, as proposed earlier by Fourier.

As mentioned in a recent paper [31], the knowledge of thermal properties can be of particular importance in the case of soils, because the role that they play to our food, shelter and well-being. McIntosh and Sharratt discuss also the features of a possible student experiment related to the conduction of heat in soils excited by a natural periodically time dependent source, namely the daily periodical oscillations in earth temperature which can be denoted as thermal waves. In my Laboratory such an experiment was designed and a device was constructed for automatic measurements of the daily time air temperature variations as well as of the daily time temperature variations at different depths beneath the soil surface [32].

Our measurements were performed using solid-state temperature sensors incorporated into a computer-controlled probe [32]. In Fig. 1 we show the hourly soil temperature measured at various depths, x , beneath the soil surface during 24 hours at Mars 6, 2002, a typical clear winter day in Havana, Cuba, as well as the hourly air temperature at the same location.

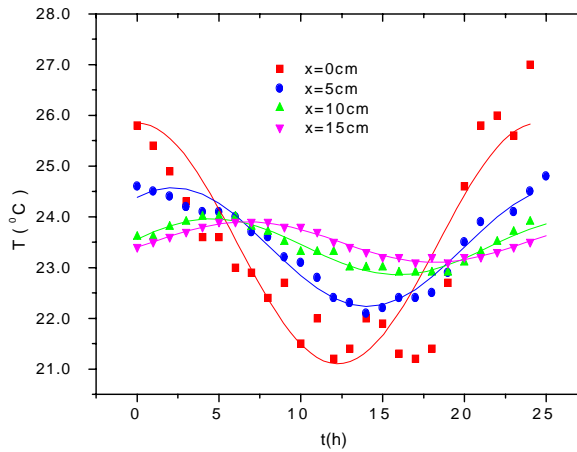


Fig. 1. Soil temperature as a function of time at different depths, x , beneath the earth surface and hourly air temperature. The solid curves represent best fits to Eq. (12). The air temperature ($x=0$) versus time curve is also represented for comparison [32].

In the figure we can see the phase shift as well as the attenuation of the temperature waves with depth, as well as their dependence on soil thermal properties, in particular its thermal diffusivity. One can easily see the attenuation of the temperature wave (i.e. the reduction in the wave amplitude) as well as the phase shift between the maximum and minimum values of the curves with depth. From the fits the obtained value for the angular frequency was $\omega = (0.256 \pm 0.008)h^{-1}$. One can observe that the variation in the air temperature is approximately sinusoidal, but that obvious differences exist: Although the period of the temperature oscillation was $T = 2\pi/\omega = (24.54 \pm 0.03)h$, the maximum and minimum of the air temperature do not occur half of an oscillation (about 12 hours) apart. The principal cause of this behavior is the deviation of the heat source from the assumed harmonic function of time. However, taking into account the good agreement between the obtained value for the period and the expected value for this magnitude, i.e. one day, our approximation can be considered as a good assumption. From the mean value of the thermal diffusion lengths, soil thermal diffusivity can be calculated using Eq. (8). We have obtained, $\alpha = (0.0022 \pm 0.0008)cm^2/s$, in agreement with previous reported values [33]. It is worth to notice that this value is an effective value for the thermal diffusivity of soil, in reality a depth dependent parameter, which was considered constant in our model. Inspired in the above mentioned work of McIntosh and Sharratt and taking into account the above described results, we have developed several exercises to introduce undergraduate students of physics and engineering in the very fascinating fields of thermal wave physics [32].

The experimental arrangement can also be useful for soil scientists, for example for recovering soil moisture from thermal properties measurements [33].

2.4 Behaviour at interfaces

As other kind of waves, thermal waves experience reflection and refraction. The characteristic coefficients for these phenomena are determined by the thermal effusivity values of the involved media using the thermal wave Eq. (12). When thermal waves propagate between the surface of two media with different thermal effusivity, then their interfere in the same way as electromagnetic, acoustic or mechanical waves do, a behaviour that can be exploited in numerous applications [1].

2.4.1 Reflection and refraction of thermal waves

Consider two regions, 1 and 2. One can show using Eq. (12), applying the boundary conditions of continuity of temperature and heat flux at the interface and performing some straightforward calculations, that the reflection and transmission coefficients for the thermal wave at the interface for normal incidence can be written as [1, 14]:

$$R = \frac{1 - b}{1 + b} \quad (13)$$

and

$$T = \frac{2}{1 + b} \quad (14)$$

where

$$b = \frac{\varepsilon_1}{\varepsilon_2} \quad (15)$$

is the ratio of the media thermal effusivities (thermal effusivity can be regarded, therefore, as a measure of the thermal mismatch between the two media).

Several applications of these results are discussed for example by Almond and Patel [1] where other thermal wave effects are also described, such as scattering at finite boundary and objects. In the next section an experiment is presented, demonstrating how the above results can be applied to describe the propagation of thermal waves through a media limited by two thermal “mirrors” experiencing interference.

2.4.2 An experiment with thermal waves: interference

Principles of Thermal wave Interference: in Fig. 2 is showed schematically a typical experimental set-up. It consists of cavity of variable length containing a sample, denoted formerly as thermal wave resonator [34-37] and then as thermal wave interferometer (TWI) [38-43].

The cavity is formed between a thin ($15\mu\text{m}$ thick) Al foil and a Photopyroelectric (PPE) sensor ($25\mu\text{m}$ thick polyvinylidene difluoride (PVDF) film with Al metalized surfaces), both 5mm in diameter. A laser light beam modulated by means of a mechanical chopper impinges on the black-painted outer surface of the Al foil, which acts as a light absorber. Following the absorption of the modulated light beam, the Al foil temperature fluctuates periodically at the modulation frequency of the incident beam thereby launching a thermal wave into the gas filled cell. The thermal waves thus generated propagate back and forth between the Al foil and the pyroelectric sensor separated by a distance L . On striking the gas-Al and gas-sensor boundaries, the thermal waves are partially reflected, and interference between the reflected and incident wave trains will set in. As discussed elsewhere [34-43] with more details the temperature rise resulting from the superposition of all arriving waves can be measured at the pyroelectric surface as a function of the gas layer thickness.

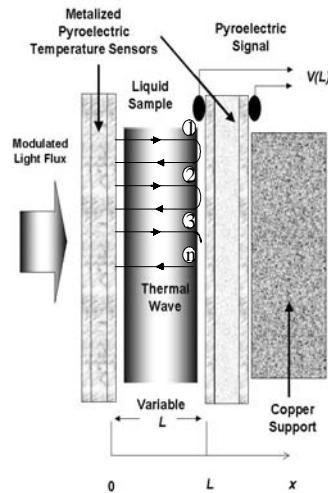


Fig. 2. Schematic view of the thermal wave interferometer described in the text, showing the principles of thermal wave interferometry (see for example Refs. 35-38).

This temperature can be estimated using the following phenomenological model [35]. Consider the situation depicted in Fig. 2. A gas layer of thickness L is sandwiched between the Al foil and a pyroelectric sensor. The outer surface of the Al film is heated by a light source of periodically modulated intensity $I_0(1 + \cos(\omega t))/2$, where I_0 is the light source intensity and $\omega = 2\pi f$ is the angular modulation frequency. The temperature distribution $T(x, t)$ within the gas region along the longitudinal x co-ordinate, following the periodic heating of the Al foil, can be obtained by solving the heat diffusion equation with the boundary condition that the heat generated at the solid surface by light absorption is dissipated in the gas by diffusion. Accordingly, this solution is similar to Eq. (12), i.e.,

$$T(x, t) = \frac{I_0}{2\varepsilon_g\sqrt{\omega}} \exp(-qx) \exp(i\omega t) = \frac{I_0}{2\varepsilon_g\sqrt{\omega}} \exp\left(-\frac{x}{\mu}\right) \exp\left[-i\left(\frac{x}{\mu} - \frac{\pi}{4-t}\right)\right] \quad (16)$$

where ε_g is the thermal effusivity of the gas, $q = (i\omega/\alpha_g)^{1/2}$, α_g is the gas thermal diffusivity and $\mu = (2\alpha_g/\omega)^{1/2}$ represents the thermal wave diffusion length in the gas.

Consider now the propagation of a plane thermal wave described by Eq. (19) through the gas medium (denoted by g) contained between the media A (corresponding to the Al foil) and P (corresponding to the PVDF sensor). The temperature at the surface $x = L$ is obtained by summing all the waves arriving at this point in the following way (for the sake of simplicity, from now on the term $\exp(i\omega t)$ will be omitted in the calculations).

$$T(L) = T_1 + T_2 + \dots + T_n = T_0 \left[e^{-qL} + R_{gA} + R_{gP}e^{-3qL} + \dots + (R_{gA}R_{gP})^n e^{-(2n+1)qL} \right] \quad (17)$$

where $T_0 = I_0/(2\varepsilon_g\omega^{1/2})$ is the gas temperature at $x = 0$, and R_{gA} and R_{gP} are the reflection coefficients at the interfaces gas-Al and gas-PVDF, respectively, as given by Eq. (13). Summing up the geometric series in Eq. (17) one gets:

$$T(L) = \frac{T_0 \exp(-qL)}{1 - \gamma \exp(-2qL)} \quad (18)$$

where we have written $\gamma = R_{gA}R_{gP}$. The temperature rise given by Eq. (30) induces an electric field between the two opposite surfaces of the PVDF sensor. The Real (in-Phase) and Imaginary (Quadrature) parts of the resulting voltage V , as well as its Amplitude and Phase, can be determined by lock-in based detection as a function of the cavity length L .

Fig. 3 shows results obtained [35] for the air-filled cavity at ambient pressure and temperature. Fig. 3a shows the In-Phase (In-P) signal as a function of the cavity length (L), whereas in Fig.3b the Quadrature (Q) signal vs. L is plotted. The solid and dashed lines represent respectively the best fit of the experimental data to the real and imaginary parts of the voltage given by the sensor, which is proportional to the temperature expressed by Eq. (18). The thermal diffusivity was taken as adjustable parameter. The value we got was $\alpha = 0.244 \pm 0.007 \text{ cm}^2/\text{s}$, which is in good agreement with reported values [30].

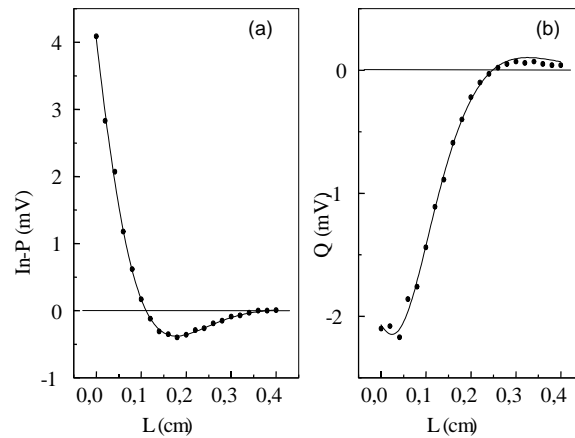


Fig. 3. In-Phase (a) and Quadrature (b) signals measured for air. The solid curves are the best-fit results to the real and imaginary parts of equation (30) respectively(after[35]).

Thermal wave interference was first discussed by Bennett and Patty [44], and was explored then by Shen and Mandelis [34] who succeeded in demonstrating the feasibility of the pyroelectric detection of a thermal wave propagating across an air gap formed between a pyroelectric sensor and a foil of another material (i.e. Aluminum) acting as the source of thermal waves. More recently the usefulness of this detection scheme for the monitoring of mass diffusion in air was demonstrated by Lima *et al* [40], as well as its capabilities to perform the thermal characterization of gases [38] and their mixtures [36, 37]. The potential use of this experimental configuration for fuel analysis, as done by the above-mentioned Brazilian group, have been recognized elsewhere [43]. This is perhaps one of the most promising applications of TWI seen nowadays. Some results concerning thermal characterization of liquids are presented next.

Measurement of thermal properties of liquids: there is an expanded demand for reliable and precise measurements of basic properties of a wide range of liquid mixtures in use today or generated by nature or modern industry, the knowledge of which can lead to a better understanding of the physical and chemical processes governing their production. The situation is particularly critical in the case of thermal properties such as thermal diffusivity and effusivity, for which only few determinations have been reported. The TWI technique can play an important role in this field, since the method is relatively simple, fast, of good accuracy, and involves small temperature oscillations, which do not affect the sample properties during their measurement.

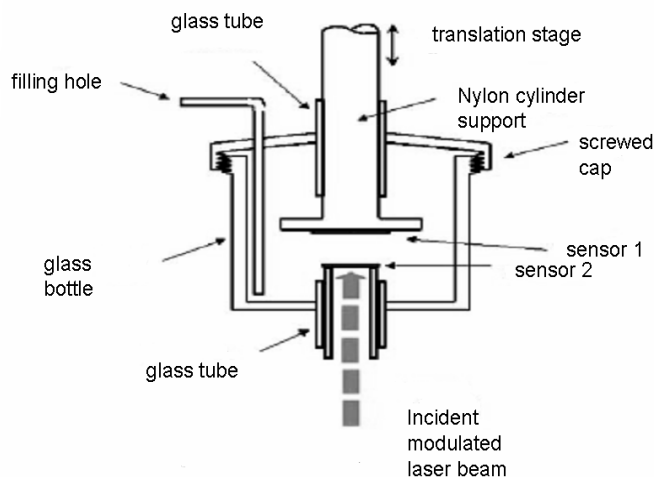


Fig. 4. Schema of a typical thermal wave interferometer designed for measurement of the thermal properties in liquids [39].

The experimental set-up reported for this purpose is similar to that shown in Fig. 2, but in this case the air filling the TWI cavity must be replaced by the investigated liquid sample [39]. For this purpose the following variant was adopted (see Fig. 4). The TWI consists of a roughly 100ml gas bottle with a cap screwed on its top. Two glass tubes of inner diameter 10mm are inserted and soldered at the bottom and the cap. The lower glass tube supports a 25 μ m thick PVDF-PPE sensor, with its outer side painted black to ensure good light absorption, on which a modulated ($f = 1Hz$) laser beam (20mW Ar-Ion) impinges generating thermal waves. It plays a role similar to that of the Al foil in the former configuration but also permits the monitoring of the laser intensity. The second glass tube guides a nylon cylinder on top of which a second PVDF-PPE sensor is glued. This is the temperature sensor. The nylon cylinder is attached to a translation stage allowing the variation of the gap between both sensors. Small holes on the top cap allow the filling of the TWI Cell with the sample, and its removal. A thin layer of silicon rubber on the lateral sides of the sensors prevents short-circuiting.

Fig. 5 shows the results obtained by Lima *et al* [39] for the amplitude of the TWI signal as a function of the cavity length for a sample of Glycerine at 25 $^{\circ}C$. The solid curve represents the best fit to Eq. (18). It is worth to notice that in the mentioned work the authors have taken into account the frequency dependence of the parameter γ , as result in the case of thermally thin pyroelectric sensors (a sample becomes thermally thin when the modulation frequency has a value so that the thermal diffusion length in the sample is greater than its thickness. In other case it becomes thermally thick).

This dependence can be obtained straightforward solving the system of heat diffusion equations for the given experimental configuration [39]. In this way thermal diffusivity and effusivity were obtained as adjustable parameters. Table 1 shows the obtained results for glycerine, distilled water and light oil. Balderas *et al* [44] have also reported measurements of thermal diffusivity of liquids using the same principle and more recently by means of PA instead of PPE detection of thermal waves.

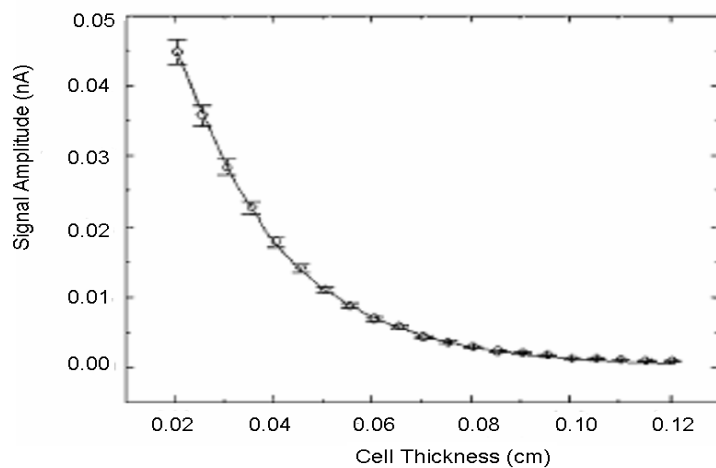


Fig. 5. Typical results obtained in the case of distilled water. Amplitude of the TWI signal as a function of the cavity length. The solid curve is the best fit to Eq. (18) [39].

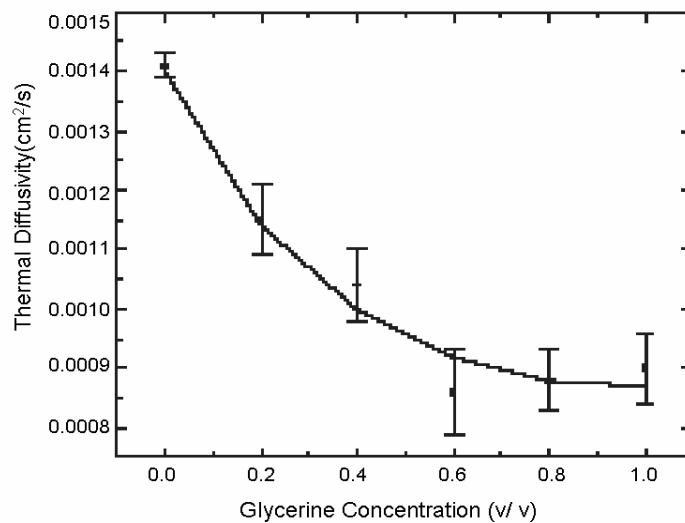


Fig. 6. Thermal diffusivity as a function of Glycerine concentration (parts per volume) in water. The solid curve is the best fit to Eq. (19) [39].

Sample	Thermal diffusivity ($10^{-4}\text{cm}^2\text{s}^{-1}$)		Thermal effusivity ($\text{W s}^{1/2}\text{cm}^{-2}\text{K}^{-1}$)	
	This work	Literature values ^b	This work	Literature values ^b
Water	15.8	14.0	0.1429	0.1582
Glycerine	9.9	9.38	0.092	0.0933
Light oli	10.0	8.8	0.0575	0.050
PVDF	-	5.4	-	0.0559

Table 1. Measured values of the thermal diffusivity and effusivity for some samples using the TWI. Literature values are also shown for comparison. (b) after reference 30.

These results suggest that the proposed TWI technique may indeed become a quite useful technique for the investigation of the thermal properties of liquids and several works in this direction are under progress. One obvious and perhaps more practical application of this method would be the case of liquid mixtures, as doing in another work by Lima *et al* [41]. The authors have measured, using the above described procedure, the thermal diffusivity of several Glycerine-Water mixtures. The results are shown in Fig. 6. They were fitted to the expression for the effective thermal diffusivity of a mixture given by the series-mixing model [45], after which this magnitude can be expressed as:

$$\alpha = \frac{\alpha_1}{\left[1 + \left(\frac{1}{\lambda} - 1\right)x\right] \left[1 + \left(\frac{\alpha_1}{\alpha_2} - 1\right)x\right]} \quad (19)$$

in which α_1 (α_2) refer to the thermal diffusivity of water (glycerine) and the parameter $\lambda = k_2/k_1$ is the glycerine-to-water thermal conductivity ratio. We note from (19) that λ is the only unknown parameter. The values of α_1 and α_2 are obtained from the extreme values of the thermal diffusivity data in Fig. 6 at $x = 0$ and $x = 1$ respectively. Thus, in carrying on the data fitting the authors have left λ as the single adjustable parameter from which, using the literature value for the water thermal conductivity, they got $k_2 = 2.4\text{mW/cmK}$ for the glycerine thermal conductivity, a value quite close to that reported in the literature [46].

3 The photoacoustic technique

In the last years scientists have witnessed the development of several PT techniques for different applications. The rest of this paper focuses on the PA technique, which, as described above, since the late seventies was incorporated to the great number of existing analytical tools. Respecting spectroscopic techniques, PAS has the advantage that it measure directly the absorbed light, which is advantageous in the case of very low absorbing samples such as the ones that will be described later. This property can also be applied for thermal characterization. The fact that the thermal diffusion length is frequency dependent is another advantage of the PA technique with respect to non-photothermal methods that can be used for depth profiling and the investigation of multiplayer samples.

This is the basis of some experiments concerning thermal effusivity measurement in liquids, where the system formed by a liquid and a reference solid sample can be regarded as a two layer one, as seen below.

3.1 The basics of photoacoustic spectroscopy

This technique looks directly at the heat generated in a sample due to non-radiant deexcitation. In a conventional arrangement, a sample is enclosed in an airtight cell and exposed to an intensity modulated light beam. As a result of the periodic heating of the sample thermal waves are generated. They propagate to the enclosed air inducing pressure oscillations at the chopping frequency that can be detected by a sensitive microphone. The PA signal depends on the way that heat is generated inside the sample and diffuses through the material. The signal depends, therefore, on the optical and thermal properties of the sample, as well as on those characterizing the non-radiant light into heat conversion mechanisms.

A great variety of PA detection schemes exist [47]. This work has dealt with open PA cell (OPC) configurations. This measurement configuration represents an open cell in the sense that the sample is mounted in the outer side of the PA air chamber, where the PA signal is detected (see Fig. 7). One of the typical experimental arrangements [48] consists on a laser, whose monochromatic light beam is modulated with a mechanical chopper and impinges onto a metallic (Al), light absorbing foil, which is fixed onto the cell with vacuum grease to seal the air chamber. The liquid sample is held on the Al support using a Teflon O-Ring, as represented in the figure.

The modulated light beam impinges the support generating a voltage signal $V(t)$ (depending on the thermal properties of the liquid sample) in the microphone whose amplitude and phase are measured as functions of frequency by means of a Lock-In Amplifier, synchronized to the chopper frequency and interfaced to a personal computer. The voltage given by the microphone is proportional to the pressure fluctuation $P(t)$ in the gas region, following the periodic heating of the sample. This kind of configuration has been applied in the past to the study of dynamic processes in liquid layers [49], measurement of thermal effusivity of solids [50], and more recently for measurement of the heat capacity per unit volume in solids [51,52], among others.

As mentioned, the experimental configuration of Fig. 7 is suitable for experiments with liquid samples. For the calculation of the PA signal one resorts to the Rosencwaig and Gerscho model [18] for its generation, after which the temperature field in the gas is calculated solving the system of heat diffusion equations in the gas, support and sample regions, and imposing the properly boundary conditions. Using the temperature value the pressure fluctuations in the PA chamber, as well as the microphone voltage response are calculated using appropriate expressions, as discussed elsewhere.

The solution of this problem is well discussed in several works, but the heat diffusion equation, in a form in which it is widely used in the photothermal science and technique (Eq. (1)) cannot be always applied when convective effects are present, as can occur nearby the frontiers of the liquid and the gas of Fig. 7 with the solid support. In what follows we will see, on the basis of the similarity theory, when such an assertion is valid. Delgado-Vasallo and Marín [53] reported such an analysis in PA experiments recently for the first time.

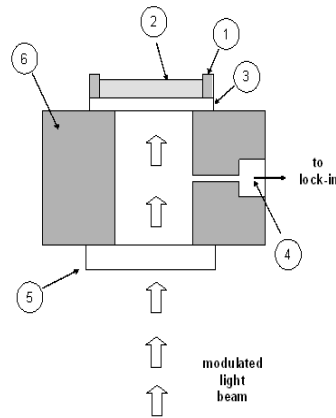


Fig. 7. Schematic view of the open photoacoustic cell described in the text. 1- Teflon O-Ring; 2- Liquid sample; 3- Al-Foil; 4- Condenser Microphone; 5- Glass window; 6- Photoacoustic cell body.

3.1.1 Differential equations describing convection in a fluid

The process of convection in an incompressible single-phase medium is described by the system of differential equations shown in Table 2 [54], featuring an infinite amount of processes. In order to single out any of them and to determine it uniquely, the equations must be supplemented by boundary and initial conditions, given a mathematical description of the considered phenomenon.

Heat transfer	$\vec{q}_{cond} = -k\nabla T$	$\vec{q}_{conv} = h\Delta T$	$T = T(\vec{r}, t)$
Energy	$\nabla^2 T - \frac{1}{\alpha} \frac{DT}{dt} = -\frac{Q}{k}, \frac{DT}{dt} = \frac{\partial T}{\partial t} + \vec{w} \cdot \nabla T, Q = Q(\vec{r}, t)$		
Motion	$\frac{Dw}{dt} = \vec{g} - \frac{1}{\rho} \nabla p + \nu \nabla^2 \vec{w}, \frac{Dw}{dt} = \frac{\partial \vec{w}}{\partial t} + (\vec{w} \cdot \nabla) \vec{w}$		
Continuity	$\nabla \cdot \vec{w} = 0$		

Table 2. Summary of the differential equations of convection for incompressible fluids in three dimensions. The meaning of the different parameters is given in the text. The symbol D/dt represents a total derivative, i.e. $D/dt = \partial/\partial t + w \cdot \nabla$

In these equations, q represents the rate of heat flux (i.e. the quantity of heat transferred through unit area per unit time normal to the isothermal surface), h is the heat transfer coefficient, \vec{w} a vector describing the fluid velocity, \vec{g} the acceleration of gravity, ρ is the fluid density, P the specific pressure of the fluid on the volume element surface and $\nu = \mu/\rho$, the quotient of the fluid viscosity to its density, is referred as the kinematical viscosity.

3.1.2 Criteria of similarity

The system of differential equations given above includes a great number of variables. Efforts to solve them analytically run into many difficulties. On the other hand, in experimental studies, in order to investigate the effect of any variable of the properties of the entire process, all the others must be maintained constant. On addition, the investigator must be sure that the results obtained by means of the given apparatus or scale model are applicable to similar processes. The theory of similarity [54] helps to resolve difficulties of this kind. In this theory the terms present in the convection equations can be united in dimensionless groups, for which one select scales of reduction. Substituting these values in the equations of Table I and after some rearrangements, one obtains other dimensionless terms with dissimilar physical parameters [55]. These terms are referred as the similarity criteria. The most important of them for the purposes of this paper is the Rayleigh number, given by

$$Ra = gl_0^3\beta\Delta T_0\nu\alpha \quad (20)$$

where l_0 and ΔT_0 are the liquid thickness and its mean temperature respectively and β is the coefficient of volumetric expansion of the fluid.

3.1.3 A criterion for neglecting convective effects

Consider a homogeneous fluid in contact with a solid (the samples support in our example), with a temperature difference ΔT in between, and suppose that there exists only free convection. Since there is a thin layer of stationary fluid at the surface of the support, Fouriers Law of heat conduction,

$$q_{cond} = -k\frac{dT}{dx} \quad (21)$$

as well as Newtons law of convection,

$$q_{conv} = h\Delta t \quad (22)$$

apply to this layer at the interface. The premise is that the one-dimensional treatment is allowed.

In accordance to Eq. (20), one gets, for a flow of heat through a thin layer of a fluid of thickness δ in contact with a solid, to the expression:

$$q_{cond} = -\frac{k}{\delta}\Delta T \quad (23)$$

where ΔT is the difference of temperature between a fluid and a solid surface. The total rate of flux through the fluid will be then given by the sum of equations (21) and (22), i.e.

$$q = \left(h - \frac{k}{\delta} \right) \Delta T = -\frac{(k - h\delta)k}{k} \frac{\Delta T}{\delta} = -\frac{k_{eq}k}{k} \frac{\Delta T}{\delta} = -\varepsilon_c \frac{k}{\delta} \Delta T \quad (24)$$

where $k_{eq} = k - h\delta$ is the so-called equivalent thermal conductivity, which accounts for the transport of heat through the passage by both conduction and convection. It is easy to show that Eq. (23), having the form similar to the Fourier's law, leads to Eq. (20) when convection is neglected. The relation $\varepsilon_c = k_{eq}/k$ characterizes the effect of convection. As shown by the similarity theory [55], this quantity is a function of the Ra number. The dependence of ε_c from Ra has been plotted from experimental data obtained by various researches [55] for several cases. One can see that for low values of the argument,

$$Ra \ll 10^3 \quad (25)$$

the value of the function is $\varepsilon_c = 1$, meaning that for those values the transfer of heat through the fluid is due only to its thermal conductivity, i.e., $k_{eq} = k$ (see Eq. (5)). For higher values of Ra the heat transfer by convection begins to play a significant role.

3.1.4 The Rayleigh number in photoacoustic experiments

One can demonstrate that the values of the Rayleigh number for a typical experimental configuration [48] are of the order of 10^{-1} and 10^{-2} for a 10^{-3} cm^3 sample of distilled water and for the air filling a 1 cm long cylindrical cavity of a 0.5 cm diameter PA chamber, respectively. For the calculation ΔT_0 was taken as 10^{-3} K , a typical mean temperature in the thin layer of stationary liquid (or gas) on the supports surface. Under these conditions, the thermal diffusion model can be applied without doubt in PA experiments with liquids.

3.2 Measurement of liquids thermal effusivity

Measurement of the thermal effusivity of liquids by PAs was reported for the first time by Balderas *et al* [56] using the compact and well recognized variant of OPC, in which the front air gap of an electret microphone, adjacent to its metalized electret membrane, is used directly as the PA chamber. However, the reported application is limited to the case of transparent liquids. More recently, and inspired in a previously reported method for thermal effusivity measurements in solids, Delgado-Vasallo and Marín have reported a PA experiment which allows the determination of this parameter for both, light absorbing and optically transparent liquid samples [57]. Their experimental configuration is the same as in Fig. 7.

The basics of the proposed methodology is the measurement of a reference sample signal (due to the Al foil along) as well as the PA signal due to the Al-liquid sample system, both as a function of the modulation frequency in a range where the Al is thermally thin and the liquid sample thermally thick. Fitting the obtained results to the expressions derived using the RG model the samples thermal effusivity can be obtained with great accuracy.

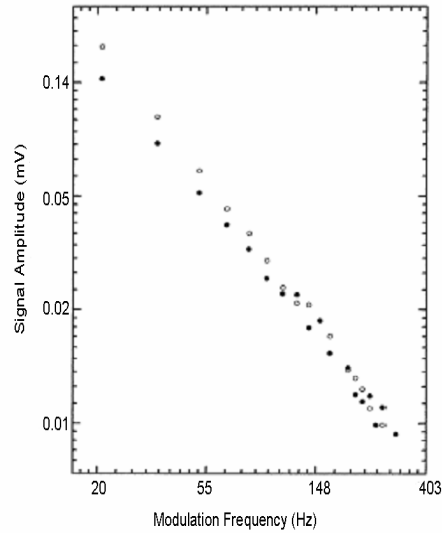


Fig. 8. Photoacoustic Signal-Amplitude vs. modulation frequency for Al (open circles) and for the Al-Water system (full circles) (after Ref. 48).

Fig. 8 shows the amplitude of the PA signal as a function of the frequency for the Al foil and for the Al-Water system. As we can see, the amplitude of the Al signal is greater than that of the Al sample system for low frequencies (up to 130Hz approximately).

This behavior is due to the fact that the heat developed by the absorption of radiation at the Al front side will flow through the foil to the sample, which acts as a heat sink. As a result the temperature (and consequently the pressure fluctuation in the PA cell) will be less than that for the situation in which no liquid is present. Table 3 shows the obtained results for several liquids, which are coherent with values reported the literature.

Liquid sample	Measured effusivity ($10^4 W s^{\frac{1}{2}} K^{-1} m^{-2}$)	Reported values ($10^4 W s^{\frac{1}{2}} K^{-1} m^{-2}$)
Petroleum	0.047 ± 0.007	0.046^a
Water	0.154 ± 0.020	0.159^a
Diffusion-pump oil	0.044 ± 0.006	0.045^b
Glycerol	0.104 ± 0.010	0.943^b
Ethanol	0.064 ± 0.009	0.058^a
Black drawing ink	0.057 ± 0.008	Not found

Table 3. Measured thermal effusivities using PA detection and literature reported values. (a) From reference 48, (b) from reference 30

3.3 Measurement of liquids thermal diffusivity

In this application, a transparent glass window, allowing the passage of the laser radiation through the liquid sample, must substitute the Al foil. As the PA signal depends on the absorbed energy, for optically transparent samples no signal will be expected. On the other hand, if the sample absorbs electromagnetic radiation, a signal must be appear whose magnitude will be proportional to the absorbed energy. This is the key idea behind the following method. Using the RG model for the generation of the PA signal, Delgado-Vasallo *et al* [57] have demonstrated that the normalized PA signal, obtained by dividing the actually signal by those corresponding to a highly absorbed sample, such as black ink, depends in a straightforward manner on the product of the optical absorption coefficient of the sample at a given wavelength and the thermal diffusion length of the sample at the used light modulation frequency. In most cases the investigated samples are transparent to the laser radiation and a colorimetric procedure is applied to give colour to the liquid, using low concentrations of the reagents so that thermal diffusivity (and consequently thermal diffusion length) becomes unaltered. For the measurement of the thermal diffusivity of ethanol, Delgado-Vasallo *et al* have resorted to methylthioninium chloride, well known as methylene blue ($C_{16}H_{18}ClN_3S$), as a colorant. This powder, when it is dissolved in ethanol, gives a broad absorption band near the excitation wavelength of 632.8nm of the used He-Ne laser. The optical absorption coefficient, β , of the solution was determined using a conventional visible light spectrophotometer. From the obtained value of the product $\beta\mu$ at a frequency of 10Hz the thermal diffusivity of ethanol was calculated as $0.79 \pm 0.15cm^2/s$, in agreement with literature values. Similar procedure can be employed for other liquids aided with properly colorimetric methods.

3.4 Determination of traces in liquids

The above principle was used by the Delgado-Vasallo *et al* to propose a method for the determination of low concentrations of solutes in liquid solutions [57, 58]. Test samples were aqueous solutions containing various concentrations of chromium (VI) (thermal properties of distilled water are well known). A series of calibration standards was prepared using a suitable calorimetric procedure, namely the 1,5-diphenylcarbazide method [59], to obtain a broad absorption band centred near the excitation wavelength used in our experiments, the 514nm line of an Ar-ion laser, whose radiation was modulated at the frequency of 1Hz by a mechanical chopper. Care must be taken in order to maintain the solution thermal properties fixed. That is achieved by the use of low concentrations of the reagents. Fig. 9 shows the calibration curve from which the Cr-VI concentration in a test sample can be determined. The detection limits in the measurements was $0.2\mu mol/L$ at the used wavelength. With the increasing human awareness regarding environmental problems, the detection of pollutant elements in water has gained importance.

In particular, the determination of Chromium (VI) in water is a field currently of considerable interest due to Cr (VI) toxicity to live organisms, including humans. Their maximum allowed value in drinking water ($0.9\mu\text{mol}/L$) [60] is well resolved in the above described experiment as well as the detection limits of Optical Spectrophotometry [61], showing the potential of PAS for sensitive spectroscopic measurements in liquids. Similar results were obtained by Lima *et al* using the Optothermal Window Method (OW) [62]. They used a very similar procedure proposed before by Helander [6].

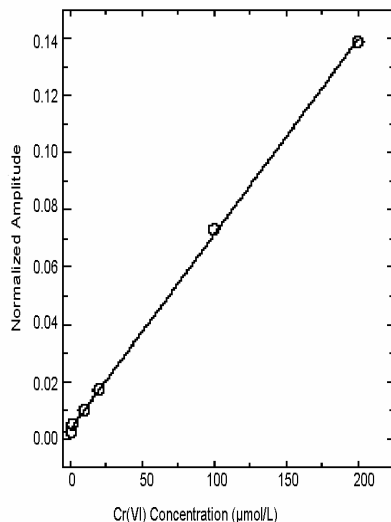


Fig. 9. Normalized Photoacoustic Signal as a function of Cr-VI concentration in water [54].

Recently Delgado-Vasallo *et al* have used the same method for the determination of the total iron content in Corn Meal [63]. The determination of this element in food is of considerable interest because several foods are currently enriched with it at proper levels in order to increase the resistance of people, after consumption, to several diseases, such as anaemia. The obtained results agree very well with those obtained using the conventional optical spectrophotometric technique, showing the possibilities of a new variant to perform this kind of measurements, with the advantage of a higher sensitivity and increment in the range of appreciable absorbance. Measurements were aided with the well-known AACC 40-41A colorimetric method. A Fe concentration of $4.2 \pm 0.4\text{ppm}$ was detected in commercial samples.

4 Concluding remarks

The conduction of heat in the presence of a periodically time-dependent source, commonly encountered in photothermal techniques, was discussed, as well as some applications related to experiments with liquids. For this purpose it has been shown, on the basis of the similarity theory, that heat convection effects can be neglected in PA experiments when the cell dimensions are such that the Rayleigh number become much lower than 10^3 . The presented analysis can be extended, with proper modifications, to other PT approaches.

Thermal wave physics has fulfilled its expectative, since its rediscover in the past century. For the characterization of liquids novel developments deserves special attention. The TWI technique, in particular, is extremely attractive, as has been recognized elsewhere [16, 45], because of its capabilities to perform thermal properties measurement and to monitoring transient processes, among others. The ancient PAS technique has also encountered novel applications concerning thermal properties determination, but most promising is its capability to detect low levels of contaminants in liquids, i.e. water. In this direction, the use of compact laser sources (for example, semiconductor lasers available on the market at relatively low cost) is an appropriate choice for enhancing the sensitivity of the proposed method for determination of trace amounts of contaminants in water. Diode-laser sources make available the possibility of constructing compact devices, suitable for in-field measurements. This work should represent a new step to understand some ways by which thermal wave physics can be applied for the quantitative characterization of liquid samples.

Acknowledgements

The author wills first thanks Prof. Helion Vargas for introducing him to the fascinating field of photoacoustic and thermal wave physics and for the helpful discussions during many years of friendly collaboration. He would also like to express his gratitude to the students and colleagues at the following institutions, where part of the research was performed: Faculty of Physics & IMRE-Havana University, Cuba, LCFIS -UENF, Brazil and CICATA-IPN, Mexico. He is also grateful to the Postdoctoral Program of CLAF-CNPq-Brazil. This work was partially supported by the Alma Mater Project 01-2001 of Havana University.

References

- [1] Almond D. P., Patel P. M., *Photothermal Science and Techniques en Physics and its Applications*, 10 Dobbsand E. R. and Palmer S. B. (Eds), Chapman and Hall, London, 1996.
- [2] Rosencwaig A., *Physics Today* 28 23(1975).
- [3] Dovici N. J., Nolan T. G. and Welmer W. A. *Anal. Chem.* 59 1700 (1984).
- [4] Tran C. D. *Photoacoustic and Photothermal Phenomena*, ed Bicanic D. (Berlin: Springer) pp 46372 1992.
- [5] Rose A., Vyas R. and Gupta R. *Appl. Opt.* 25 4626 (1986).
- [6] Helander P. J. *Photoacoust.* 1 103 (1982).
- [7] Chirtoc M., Tosa V., Bicanic D. and Toris P. Ber. Bunsenges. *Phys. Chem.* 95 766 (1991).
- [8] Dadarlat D., Bicanic D., Visser H., Mercuri F. and Frandas A. *J. Am. Oil Chem. Soc.* 72 273 (1995).

- [9] Dadarlat D., Bicanic D., Visser H., Mercuri F. and Frandas A. *J. Am. Oil Chem. Soc.* 72 281 (1995).
- [10] Dadarlat D., Riezebos K. J., Bicanic D., Van den Berg C., Gerkema E. and Surducun V. *Adv. Food. Sci. (CMTL)* 20 27 (1998).
- [11] Moroka N., Yarai A. and Nakanishi T. *Japan. J. Appl. Phys.* 34 2579 (1995).
- [12] Mandelis A. and Zver M. M. *J. Appl. Phys.* 60 4421 (1985).
- [13] Chirtoc M. and Mihailescu G. *Phys. Rev. B* 40 9606 (1989).
- [14] Bein B. K. and Pelzl J., *Analysis of Surfaces exposed to Plasmas by Nondestructive Photoacoustic and Photothermal Techniques in Plasma Diagnostics*, Surface Analysis and Interactions (Academic, New-York), 1989.
- [15] Although the most experimental applications are modelled using the well known parabolic heat diffusion equation, the potential use of high intensity and ultra-short duration laser pulses, as well as the possibility of performing such experiments at low temperatures, can lead to situations where such physical-mathematical formalism is no longer valid and one must resort to the use of a heat diffusion equation of hyperbolic kind. Hyperbolic heat transport in photothermal experiments was described recently in Marín E., Marín-Antuña J. and Díaz-Arencibia P. *Eur. J. of Phys.* 23, 523, 2002.
- [16] Vargas H. and Miranda L. C. M. *Rev. Sci. Instrum.*, 74 794 (2003).
- [17] ngström A. *J. Ann. Physik. Lpz.* 114 513 (1861).
- [18] Rosencwaig A. and Gersho A. *J. of Appl. Phys.* 47 64 (1976).
- [19] Bell A. G. *Am. J. of Sci.* 20 305 (1880).
- [20] Röntgen W. K. *Ann Phys Lpz.* 12 155 (1881).
- [21] Tyndall J. J. *Proc. R. Soc. London* 31 308 (1881).
- [22] Lord Rayleigh *Nature* 23 274 (1881).
- [23] Viengerov M. L. *Dokl. Akad. Nauk. SSSR* 19 687 (1938).
- [24] Mandelis A. *Phys Today* 53 29 (2000).
- [25] Fourier J. B. *Analytical theory of Heat*, translated by A. Freeman (Encyclopedia Britannica, Inc., Chicago), 1952.
- [26] Poisson S. D. *Théorie Mathématique de la Chaleur* (Bachelier, Imprimeur-Libraire, Paris), 1855.
- [27] Mandelis A. *Diffusion-wave fields: mathematical methods and green functions.* (Springer-Verlag New York) 2001.
- [28] Carslaw H. S. and Jaeger J. C. *Conduction of Heat in Solids* (Oxford Univ. Press, London), 1959.

- [29] Salazar A. *Eur. J of Phys.* 24 351 (2003).
- [30] Touloukian Y. S. (Ed.), Thermophysical Properties of Matter. *The Thermophysical Properties Research Center Data Series*, (IFI/Plenum Press, New York), 1970.
- [31] McIntosh G. and Sharratt B. S. *The Phys. Teach.* 39 458 (2001).
- [32] Jean-Baptiste L. E., *Estudio de la propagación de ondas de temperatura en suelos*, Master Thesis in Physics Education, Universidad de La Habana, La Habana, 2002. (submitted to Revista Mexicana de Física)
- [33] Hanks R. J., *Applied soil physics. Soil water and temperature applications*, 2nd ed., (Springer-Verlag, New York), 1992. see also Fuhrer O. Inverse Heat Conduction In Soils A New Approach Towards Recovering Soil Moisture From Temperature Records Diploma Thesis Climate Research ETH, Zurich ETH Zurich, Dept. Physics March 2000. <http://iacweb.ethz.ch/staff/fuhrer/publ/dipl/>
- [34] Shen J. and Mandelis A *Rev. Sci. Instrum.* 66 4999 (1995).
- [35] Lima J. A. P., Marín E., Cardoso S. L., Takeuty D., da Silva M. G., StHEL M. S., Rezende C. E., Gatts C. N., Vargas H. and Miranda L.C.M., *Rev. of Sci. Inst.* 71 2928 (2000).
- [36] Lima J.A.P., Marín E., Cardoso S. L., da Silva M.G., StHEL M.S., Vargas H. e Miranda L.C.M.. *Rev. Sci. Instrum.* 72 1580 (2001).
- [37] Marin E., Lima J. A. P., da Silva M. G., StHEL M. S., Cardoso S. L. and Vargas H. *Analytical Sciences* 17 475 (2001).
- [38] Lima J.A.P., Marín E., da Silva M. G., StHEL M. S., Schramm D. U., Cardoso S. L., Vargas H. y Miranda L. C. M. *Measurement Science and Technology*, 12 1949 (2001).
- [39] Lima J.A.P., Marín E., Correa O., Cardoso S. L., da Silva M.G., Vargas H. y Miranda L.C.M.. *Meas. Science and Technology* 11 1522 (2000).
- [40] Lima J. A. P., da Silva M. G., StHEL M. S., Cardoso S. L., Vargas H., Marin E. and Miranda L. C. M. *Rev. of Sci. Inst.* 74 433 (2003).
- [41] Lima J.A.P., Marín E., Massunaga M.S.O., Correa O., Cardoso S.L., Vargas H. y Miranda L.C.M. *Applied Physics B: Lasers and Optics* 73 151 (2001).
- [42] Bennett C. A. and Patty R. R. *Appl. Opt.* 21 49 (1982).
- [43] Burgess D. S. *Photonics Technology World*, March 2004.
- [44]. Balderas-López J. A, Mandelis A. and García J. A. *Anal. Science* 17, 519 (2001).
- [45] Tye R.P.: *Thermal Conductivity* (Academic, New York), 1969.
- [46] Whitaker S. *Elementary Heat Transfer Analysis* (Pergamon, New York), 1976

- [47] Vargas H. and Miranda L. C. M. *Physics Reports* 161 43 1988.
- [48] O. Delgado-Vasallo and E. Marin J. *Phys. D: Appl. Phys.* 32, 593 (1999).
- [49] Miranda L C M and Cella N *Phys. Rev. B* 47 3896 (1993).
- [50] Veleva L., Tomas S. A., Marín E., Cruz-Orea A., Delgadillo I., Alvarado-Gil J. J., Quintana P., Pomés R., Sanchez F., Vargas H. y Miranda L. C. M. *Corrosion Science* 19 1641 (1997).
- [51] Gutiérrez-Juárez G., Vargas-Luna M., Camacho-Espinosa J. J., Sosa M., González-Solís J. L., Bernal-Alvarado J. and Alvarado-Gil J. J. *Rev. Sci. Instrum.* 74 845 (2003).
- [52] Delgado-Vasallo O., Peña-Rodríguez G., Marin E., Peña J. L., Díaz Gongora J. A. I. and Calderón A. *Journal de Physique IV* (submitted for publication).
- [53] Delgado-Vasallo O. and Marín E. *Journal de Physique IV* (submitted for publication).
- [54] Kutateladze S. S., *Analysis of Similarity and physical models* (Nauka: Novosibirsk), 1986 (in Russian).
- [55] Mikheeva I. M. *Heat Transfer and Thermal Simulation* (Teploperedacha i teplovoe modelirovanie), (USSR Acad. Scient.), 1959 (in Russian).
- [56] Balderas-López J. A., Acosta-Avalos D., Alvarado J. J., Zelaya-Angel O., Sanchez-Sinencio F., Falcony C., Cruz-Orea A. and Vargas H. *Meas. Sci. Technol.* 6 1163 (1995).
- [57] Delgado-Vasallo O., Valdés A.C., Marín E., Lima J.A.P., da Silva M.G., Sthel M.S., Vargas H y Cardoso S. L. *Meas. Sc. Technol.* 11 412 (2000).
- [58] Lima J.A.P., Marin E., Cardoso S. L., Delgado-Vasallo O., da Silva M.G., Sthel M.S., Gatts, C.E.N., Mariano A., Rezende C.E., Ovalle A.R.C., Suzuki M.S. y Vargas H. *Anal. Sciences* 17 530 (2001).
- [59] Clesceri L.S., Greenberg A.E. and Eaton A.D. (Eds.) *Standard Methods for the Examination of Water and Wastewater* (American Public Health Association: Washington DC) 1998, pp. 4-146.
- [60] Water Quality Criteria (*Ecological Research Series*) (Washington, DC: EPA) 1972.
- [61] Seidel B. S. and Faubel W. *Opt. Enging.* 36 469 (1997).
- [62] Lima J.A.P., Marín E., Cardoso S. L., da Silva M.G., Sthel M., Costa C.G.S., Mariano A., Rezende C.E., Ovalle R.C., Susuki M.S. y Vargas H. *International Journal of Envirommental Analytical Chemistry* 76 331 (2000).
- [63] Delgado-Vasallo O., Peña J. L., San Martín Martínez E., Calderón A., Peña-Rodríguez G., Jaime Fonseca M. R. and Marín E. *Anal. Sciences*, 19, 599 (2003).